Solidification enhancement of phase change material in a triplex tube latent heat energy storage unit using longitudinal-parabolic fins

Farhad Moheiseni, Zahra Mehrdoost[1]

Department of Mechanical Engineering, Ahvaz Branch, Islamic Azad University, Ahvaz, Iran

Abstract

This paper numerically investigates the solidification performance improvement of phase change material in a triplex tube latent heat thermal energy storage unit by introducing an innovative longitudinal-parabolic fin. A numerical model based on the enthalpy-porosity approach is employed to simulate the discharging process. Simulation results reveal that the longitudinal-parabolic fins outperform the conventional straight fins in effectually increasing the phase change performance of latent heat thermal energy storage unit. The complete discharging time of triplex tube latent heat thermal energy storage unit with the proposed fin reduced up to 38.5% compared to that of the unit with straight fins. The study also investigates the influence of geometric parameters of the designed fin to achieve superior phase change material discharging efficiency. Effects of radial pitch and angular pitch of the longitudinal-parabolic fins on energy discharge time are studied through examine various cases under the constant total fins volume. Results infer that the radial pitch of parabolic fins has a moderate impact on solidification time improvement, while the angular pitch has a remarkable impact on reducing energy discharging time. Decreasing the angular pitch from 120° to 60° reduces the solidification time by 52.3%. The maximum of saving discharge time for the most efficient fin design is 61.8% in comparison with straight fins.

Keywords: Longitudinal-parabolic fin, Thermal energy storage, Solidification, PCM

[1]corresponding author: za.mehrdoost@iau.ac.ir

1. Introduction

The increasing energy demand has led researchers to focus on effectively harnessing renewable energy sources and optimizing current energy systems. Thermal energy is obtained from different renewable energy resources like solar, nuclear power, and geothermal. Most renewable energy resources suffer from the drawback of inferior stability, which makes thermal energy storage crucial for effectively harnessing renewable energy. Thermal energy is stored in form of thermo-chemical heat, sensible heat, or latent heat. Latent heat thermal energy storage is preferred over sensible heat storage owing to its higher storage capacity, compactness, and constant temperature operation [1-3].

Latent heat thermal energy storage systems (LHTES) employ phase change material (PCM) to store and release high amount of thermal energy when undergoing phase transition [4,5]. However, LHTES systems pose major challenges due to inferior thermal conductivity of PCMs that hampers the rate of phase change [6,7]. Thermal performance enhancement of LHTES systems is performed through various techniques, including the use of nanoparticles [8-11], metal foam [12-14], fins [15-17] and composite phase change materials [18,19]. Among these methods, adding high conductive fins have emerged as the most prevalent approach for effective enhancement of energy storage efficiency [20]. Various configurations of fins have been presented in the literature with different parameters that have been adjusted to find the optimal configuration to increase heat transfer in LHTES systems. Sciacovelli et al. [21] introduced a Y-shaped fin design to increase efficiency of LHTES system and found that these fins are more efficient than straight fins. They optimized the configuration of fins by combination of the response surface method and CFD simulation and observed that the efficiency improves by adding the bifurcations in the fins. Sheikholeslami et al. [22] designed a new fin based on the snowflake structure. Their finding demonstrate that the inclusion of snowflake-shaped fins accelerate discharging process of the storage unit up to 1.5 times when compared to straight fins. Aly et al. [23] analyzed the potential of longitudinal corrugated fins for increasing the PCM discharging rate in LHTES unit. Numerical findings demonstrated that corrugated fins shortened the full discharging time up to 30-35% in comparison with straight fins. Zhang et al. [24] proposed helical fins to accelerate the PCM charging rate in thermal energy storage system. They found that the best thermal performance in vertical LHTES can be achieved by double helical fin, and in a horizontal LHTES with quadruple helical fin. Compared with traditional longitudinal fins, the total charging time declined up to 31% and 10% in vertical and horizontal systems. Huang et al. [25] studied the

melting/solidification process of the LHTES unit equipped with fractal tree-shaped fins. Numerical findings revealed that the full PCM melting and solidification times declined up to 34.5% and 49.4% compared to rectangular fins. Yao and Huang [26] proposed longitudinal triangular fins to enhance discharging performance of triplex-tube TES system. They concluded that the solidification time decreased up to 30.98% compared to typical rectangular fins. Huang and Yao [27] proposed a new trapezoidal longitudinal outer fin distributed by Fibonacci sequence and analyzed the effect of different longitudinal fin arrangements on solidification performance. Numerical results illustrated that the discharging time using modified trapezoidal fin is shortened up to 45.28% compared with the quadrilateral fin. Patel et al. [28] studied PCM's heat transfer enhancement using combined eccentricity and longitudinal fin. Among the eccentricities of -15mm to +15mm, the most effective eccentricities were +10mm in melting and -3mm in solidification with 27.63% and 12.82% reduction in phase change time, respectively. Zheng et al. [29] proposed an arrow-shaped fin structure based on fast optimization algorithm to increase the discharging performance of LHTES system. Results showed the arrow-shaped fins could decrease the full solidification time up to 52% compared to the traditional Y-shaped fins. Lijun et al. [30] investigated discharging efficiency enhancement of LHTES device using eccentric fractal finned tube and concluded that the complete discharging time was declined up to 41.2% compared with eccentric rectangular fins. Zhang et al. [31] proposed the combination of novel branch-structured fins and nanoparticles to enhance the solidification performance of PCM in a triple-tube heat exchanger. They concluded that the discharging time is reduced up to 10.3% for nanoparticles only and 83% for fin only. Ma Zhang et al. [32] summarized the research about the heat transfer improvement of PCM using fin tubes. They compared different fin structures including rectangular fin, spiral fin, annular fin, plate fin and dendritic fin. They found that rectangular fins usually show better performance that annular fins and innovative fins are generally better than rectangular fins. Amini and Abbasirad [33] proposed an innovative longitudinal arc fin to increase charging efficiency of LHTES device. Numerical results demonstrated that the optimized fin configuration declined the full charging time by 67.7% compared to rectangular fins. Li et al. [34] worked on the influence of leaf-shaped longitudinal fins on the charging efficiency of PCM-based shell and tube storage device. They evaluated the influences of fin geometry parameters and showed that by increasing the sub-branch length of leaf-shaped fins, charging process accelerated and more uniform heat transfer achieved. Tavakoli et al. [35] proposed sinusoidal fins for performance improvement of LHTES system. They conducted a comprehensive sensitivity analysis and

observed that the melting rate accelerated up to 62% in comparison with straight fins. Oskouei and Bayer [36] executed experimental and numerical studies on energy storage improvement in a LHTES system using Fibonacci-inspired fins. Their results inferred that the complete solidification and melting time declined up to 45% and 20% in comparison with longitudinal fins. Zheng et al. [37] designed a spiderweb-shaped fin for energy release improvement of LHTES unit. They optimized geometrical parameters of the proposed fin and found that the full discharging time decreased up to 88.9% compared to rectangular fins. Boujelbene et al. [38] explored the impact of twisted fins on PCM melting and solidifying rates in a LHTES system and demonstrated the melting and solidification rates by twisted fins improved by 10% and 14% in comparison with straight fins. Li et al. [39] employed structural-optimized spiral fins to increase the performance of heat storage in LHTES unit. Numerical results illustrated that thermal storage system with denser, higher, and thicker bottom fin demonstrates a faster charging rate.

After conducting a thorough literature review, it is apparent that altering the fins configuration could effectively improve thermal performance of LHTES systems and significant achievements have been made in practical applications. Nevertheless, there is still much space for further improvement in energy storage performance of LHTES units by exploring more innovative fin configurations. This paper innovatively presents a new longitudinal-parabolic fin and conducts a detailed numerical investigation to explore the influences of different geometrical parameters of the designed fin on the discharging efficiency of the PCM in a triplex tube LHTES unit. The longitudinal-parabolic fin will be evaluated against the conventional straight fin to find out the superior thermal performance of the innovative fin. While total surface area of fins are kept constant, several cases with different fin's geometric parameters including radial pitch and angular pitch are designed to determine the most efficient fin layout to achieve highest thermal energy release efficiency.

2. Model description

The physical model entails a PCM-based triplex tube LHTES unit with longitudinal-parabolic fins, as depicted in Fig. 1. The water as HTF passes in the inner tube and in the region between the middle and outer tubes, and the PCM is filled in the annulus region among the inner and middle tubes. The computational domain is regarded as two-dimensional model due to the smaller temperature gradient in axial direction than the radial direction. The space among the inner and middle tubes of the storage system is the simplified domain for the

simulation (Fig. 1(b)). The diameters of the inner and middle tubes are 20 mm and 70 mm, in respective. The solid material for the tubes and fins is copper and RT35 is chosen as the PCM. The thermophysical properties of the involved materials are displayed in Table 1 [40].

The longitudinal-parabolic fins are designed to increase the efficiency of the PCM-based thermal energy storage unit during the discharge phase. The proposed fin consists of a quadrilateral fin as the base of the structure and three parabolic sub-fins with different heights that are connected to the base fin. To assess the longitudinal-parabolic fins, their thermal performances are compared to that of traditional straight fins. The influence of geometrical parameters of longitudinal-parabolic fins including radial pitch (space between sub-fins in the radial direction) and angular pitch (the angle between two fins in circumference direction) are evaluated. Nine different cases are analyzed in this study. The fins are designed so that the total cross-section area maintains fixed in all cases to enable the comparability of the system with different fin configurations. Accordingly, the amount of PCM remains constant in all cases. Fig. 2 depicts the geometrical parameters of the longitudinal-parabolic fins including length (H) and width of the quadrilateral fin (w), heights (L_1, L_2, L_3), root width (w_f) and radial pitches (S_1, S_2, S_3) of the parabolic sub-fins, and angles between the fins (α). The parabolic equation of sub-fins is also shown in Fig. 2. The coefficient $w_f / 2L^2$ determines the steepness and direction of the parabola. The value of L influences how wide or narrow the parabola is. The details of the geometrical characteristics for each case are listed in Table 2.

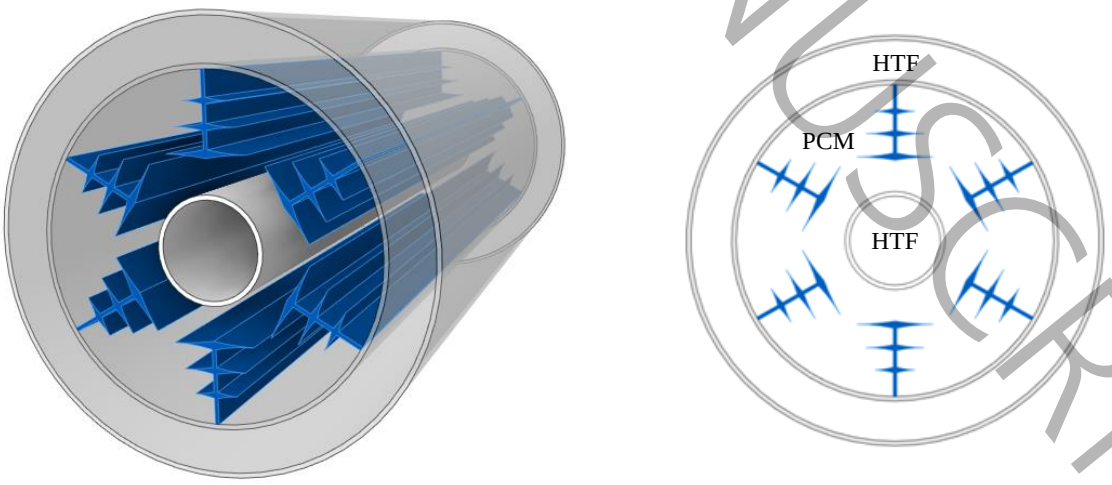

(a) (b)

Fig. 1. The triplex tube LHTES unit: (a) 3D schematic view, (b) 2D cross section.

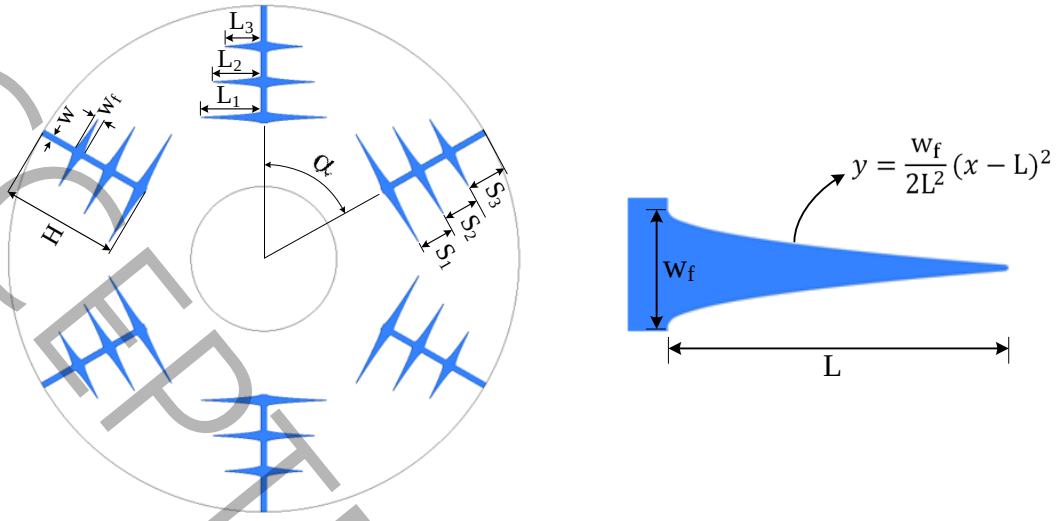

Fig.2. Two-dimensional computational domain.

Table 1
Thermo-physical properties [40]

Properties	Materials	
Name, Symbol (unit)	Paraffin (RT35)	Copper
Liquidus Temperature, T_l (K)	308	–
Solidus Temperature, T_s (K)	302	–
Density, liquid, ρ_l (kg/m^3)	880	–
Density, solid, ρ_s (kg/m^3)	760	8798
Specific heat, liquid, C_{p_l} (J/kgK)	1800	–
Specific heat, solid, C_{p_s} (J/kgK)	2400	381
Thermal conductivity, k (W/mK)	0.2	387.6
Dynamic viscosity, μ (kg/ms)	0.023	–
Latent heat of fusion, L_f (J/kg)	170000	–
Thermal expansion Coefficient, β (1/K)	0.0006	–

Table 2
Geometric dimensions of all cases (all dimensions are in mm).

Case	H	w	w_f	L_1	L_2	L_3	S_1	S_2	S_3	α/°
Base Case	20	2.75	-	-	-	-	-	-	-	90
Case 1	20	1	2	10	8	6	6	6	8	90
Case 2	20	1	2	10	8	6	4	4	12	90
Case 3	20	1	2	10	8	6	6	4	10	90
Case 4	20	1	2	10	8	6	10	4	6	90
Case 5	20	1	2	10	8	6	4	10	6	90
Case 6	20	1	2	10	8	6	6	10	4	90
Case 7	22	1.16	2.3	12	9	7	7	7	8	120
Case 8	16	0.8	1.5	8	6	4	5	5	6	60

3. Mathematical modeling

3.1. Governing equations and numerical implementation

PCM solidification process was numerically simulated via the enthalpy-porosity method [41]. This method does not explicitly track the common solid-liquid interface, rather the computational region is considered to be a porous zone. The porosity is identical to the PCM liquid fraction which is calculated using the enthalpy balance, and changes from zero to one in the mushy zone. The following assumptions were considered for the numerical simulation:

- The flow of PCM is transient, incompressible and laminar.
- The PCM's thermophysical properties, except for its density, are considered temperature independent.
- The PCM's volume change caused by phase transition is neglected.
- Temperature changes in the HTF are neglected.
- Boussinesq approximation is employed for buoyancy effect.
- Heat loss to the environment is insignificant.

The equations governing the PCM solidification process are defined by continuity, momentum and energy equations [42]:

$$\frac{\partial u_i}{\partial x_i} = 0 \tag{1}$$

$$\rho \frac{\partial u_i}{\partial t} + \rho \frac{\partial u_i u_j}{\partial x_j} = -\frac{\partial p}{\partial x_i} + \mu \frac{\partial^2 u_i}{\partial x_j^2} + \rho\beta(T - T_{ref}) g_i + S_i \tag{2}$$

$$\rho \frac{\partial H}{\partial t} + \rho \frac{\partial u_i H}{\partial x_i} = \frac{\partial}{\partial x_i} k \frac{\partial T}{\partial x_i} \tag{3}$$

where u_i, ρ, μ, p, g_i, k and T are fluid velocity, density, dynamic viscosity, pressure, gravity, thermal conductivity and temperature. Total enthalpy (H) of PCM is given by:

$$H = h + \Delta H \tag{4}$$

$$h = \int_{T_{ref}}^{T} C_p dT + h_{ref} \tag{5}$$

in which h_{ref} is the sensible enthalpy correspond to the reference temperature T_{ref}, and C_p indicates the specific heat capacity. The latent heat is stated as:

$$\Delta H = \lambda L_f \tag{6}$$

where L_f refers to the latent heat. λ is the melting fraction expressed as:

$$\lambda = \begin{cases} 0 & if \;\; T \le T_s \\ \dfrac{T - T_s}{T_l - T_s} & if \;\; T_s < T < T_l \\ 1 & if \;\; T \ge T_l \end{cases} \tag{7}$$

The subscripts 'l' and 's' indicate the PCM liquidus and solidus states, respectively. The momentum source term S_i is defined as [43]:

$$S_i = A_m \frac{(1-\lambda)^2}{\lambda^3 + \varepsilon} u_i \tag{8}$$

Where A_m is the mushy constant which varies from 10^4 to 10^7, and is set to 10^5 in this study [44]. ε represents a small value to avoid zero denominator when $\lambda = 0$.

Ansys-Fluent software is applied for numerical simulations. The finite volume method with transient pressure-based solver is applied. The momentum and energy equations are discretized using the QUICK scheme. The PRESTO algorithm used for pressure correction equation. The SIMPLE scheme is applied to couple the pressure and velocity. The relaxation

factors for pressure, momentum, liquid fraction and energy are 0.3, 0.7, 0.9 and 1, in respective. Convergence criterion was set at 10^{-4} in the continuity and momentum equations, and 10^{-6} in the energy equation.

3.2. Boundary and initial conditions

At the onset of the discharging process, the temperature of the system is initialized as 320 K. The surfaces of the both inner and outer tubes are maintained at constant temperature at 250 K that is lower than the PCM solidus temperature. Moreover, no-slip condition imposed at the walls.

3.3. Grid and time step independence study

Grid independency in the numerical solution was examined through different grid sizes and the result is shown in Fig. 3(a). Unstructured grid was adopted for better compatibility. The complete solidification time for six different grids with 41371, 57522, 103451, 233530, 361045 and 527092 cells were studied. The results illustrated that increasing the elements number from 103k to 527k does not result in considerable variation in the outcomes. Hence, a grid size of 103451 elements was selected to consider solution accuracy and computational time. The generated grid is shown in Fig. 3(b).

Time step independence analysis was also investigated. Fig. 4 shows the complete solidification time and solid fraction among different time steps. It is apparent that the solid fraction curves are almost identical for time steps less than 0.2s. Thus, to efficiently save computational cost and accurate prediction, the time step of 0.2s is assumed for the next simulations.

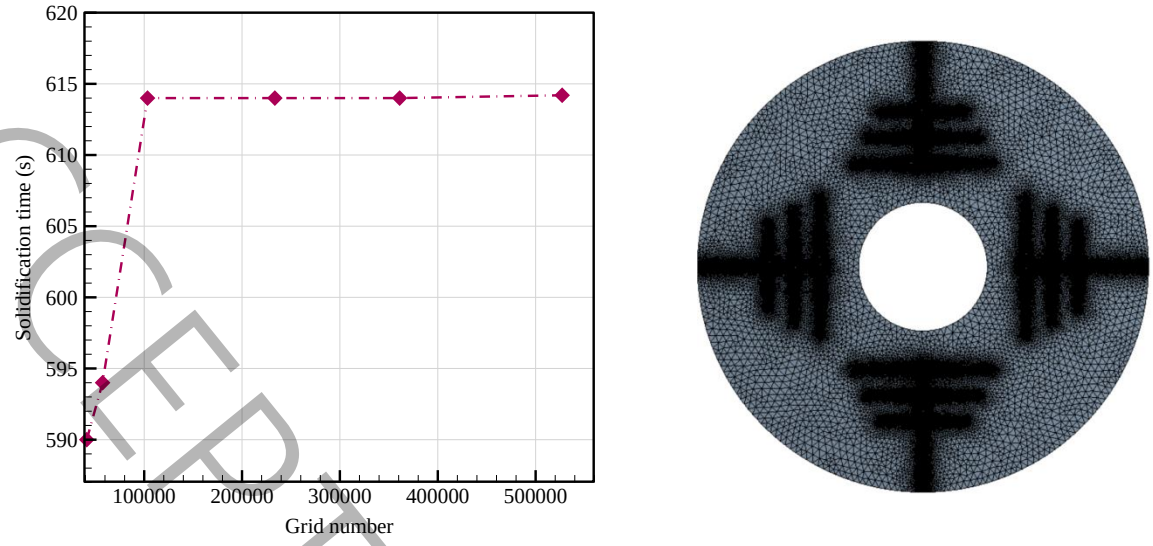

(a) (b)

Fig. 3. (a) Grid size independence verification, (b) the computational grid.

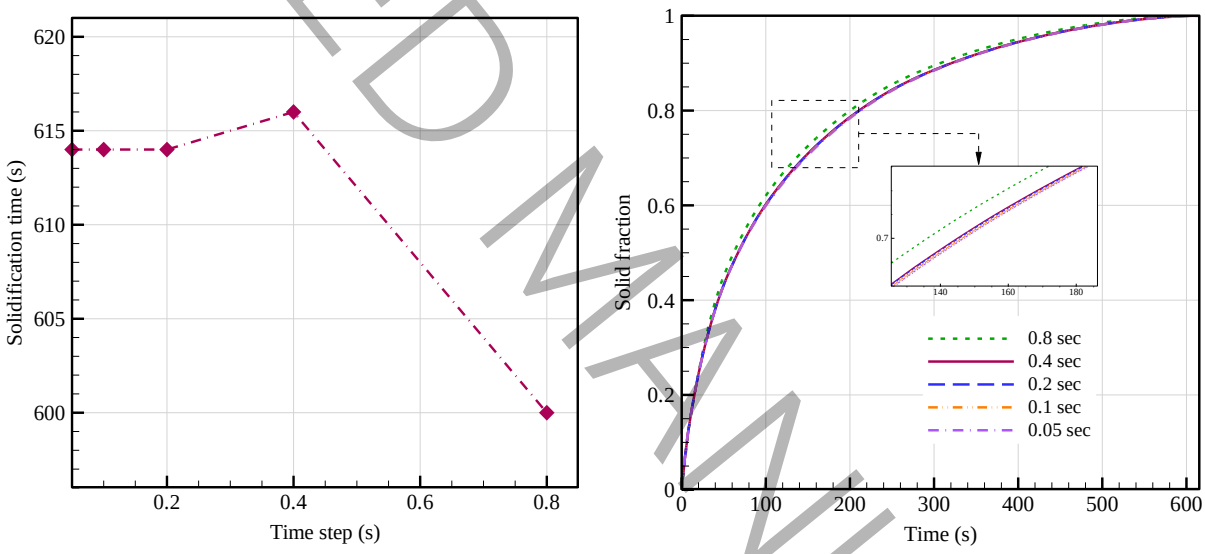

(a) (b)

Fig. 4. Time step independence study.

3.4. Numerical modeling validation

The current numerical approach has been validated through comparison of the simulation results with experimental analysis carried out by Al-Abidi et al. [45]. In their experiment, the PCM phase change process in a thermal storage enclosure with straight fins was studied. Fig. 5 shows a comparison of the PCM mean temperature throughout discharging process for the numerical prediction and experimental data. The comparison indicates that the current prediction agrees well with the reference work. The maximum relative error among the

numerical prediction and the experimental measurements is 5%, which verifies the current numerical approach.

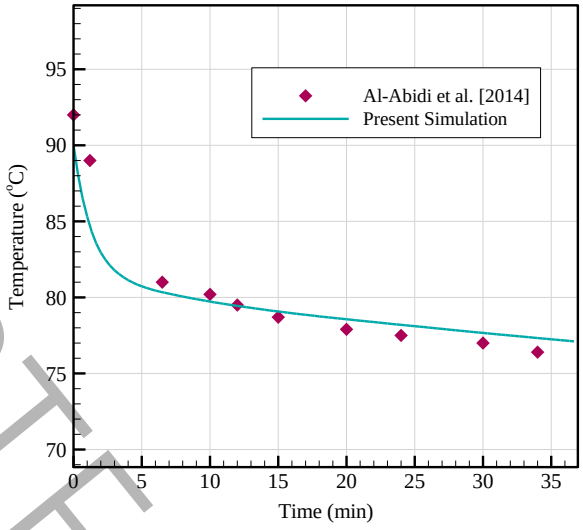

Fig. 5. Comparing numerical predictions with experimental work in [45].

4. Results and discussion

Numerical simulation results are presented in four subsections. The first subsection compares the performance of longitudinal-parabolic fins and conventional straight fins. The second subsection investigates the impact of fin radial pitch on the PCM discharging process. The third subsection examines the effect of angular pitch on solidification performance. The fourth subsection compares the full solidification time for all the designed cases. In all the cases, total cross-sectional area of all fins holds fixed. Initially, the PCM is in liquid state and its thermal energy is gradually transferred to the cold HTF, which has a less temperature than the PCM's solidification temperature.

4.1. Effect of fin shape on discharging process

In this subsection, the influence of designed fin configuration on the solidification process is compared with those of traditional straight fins as the base case. Fig. 6 represents the PCM liquid fraction contours of two fin configurations at various times. As observed in the figure, at initial solidification stage, narrow solidified layers of PCM starts to form around the fins and HTF tube walls by natural convection heat transfer. As time goes on, the solidification zone gently expands by releasing more heat from the PCM to the cooling boundaries. As time progresses and the solidified layer increased, conduction is taken place to further propagate the solid regime. The flow of the liquid PCM is decreased and natural convection becomes

insignificant, and conduction heat transfer becomes the predominant mode in discharging process.

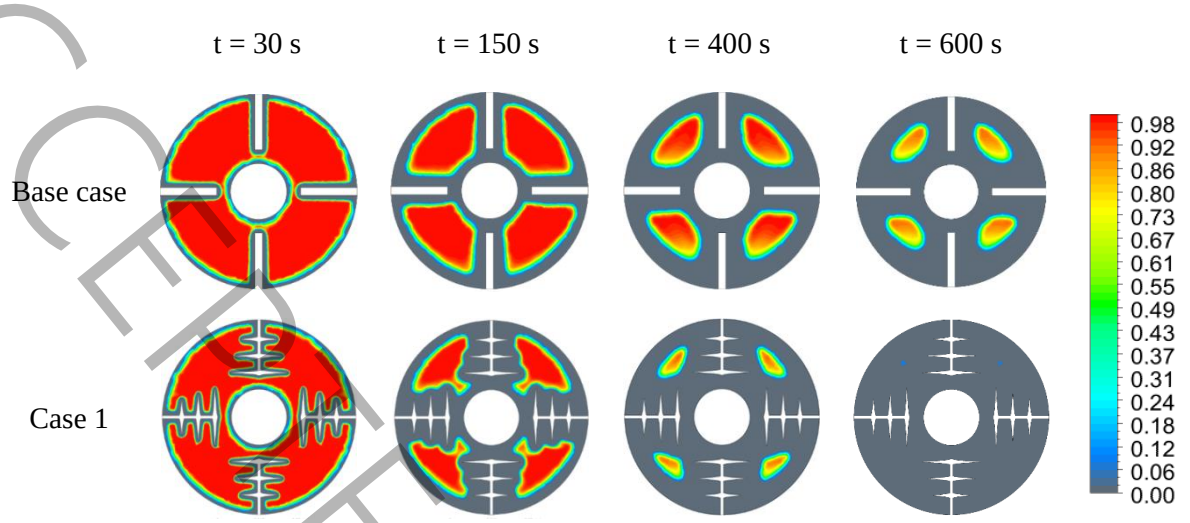

Fig. 6. Contour plot of liquid fraction for the straight fins and longitudinal-parabolic fins.

It is observed from Fig. 6 that using new fin configuration significantly improved the PCM solidification rate in comparison to the straight fins. The solid fraction of longitudinal-parabolic fins is greater than that of the straight fins during every time intervals. The higher amount of solidified PCM is due to the more extensive heat transfer surface of the longitudinal-parabolic fin configuration, leading to increased heat removal from the PCM and more expansion of solid layers in the voids between fins. Fig. 7(a) displays the PCM solid fraction against time for two different fin shapes. It is observed that in the initial stage the solid fraction increases rapidly due to direct contact of liquid PCM and cold surfaces which facilitates faster heat transfer. As time proceeds and the solidified layer increased, conduction is happened among the solid and its adjacent liquid PCM that decelerate the solidification rate owing to inferior thermal conductivity of PCM. The discharging process of the base case with straight fins is slower than that of Case 1. The discharging time of the conventional straight fins is 986s, while the full solid fraction of longitudinal-parabolic fins is reached within 606s. Fig. 7(b) illustrates the PCM mean temperature variations over time for two fin shapes. It is observed that the average temperature curve of two cases decreases rapidly at early stages of the solidification owing to higher rate of heat transfer caused by a larger temperature gradient. After that, the average temperature curves descend with a decreasing slope by declining the rate of heat transfer as the temperature gradient diminishes. The PCM mean

temperature of Case 1 with longitudinal-parabolic fins is lower than that of the straight fins case owing to different heat transfer behavior of two cases as explained above.

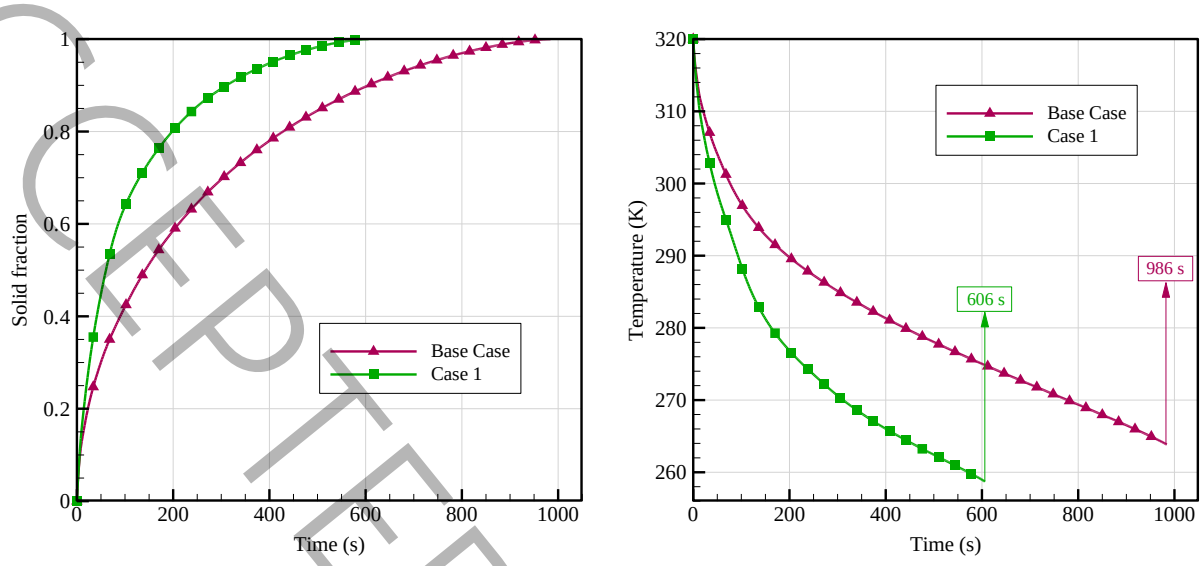

(a) (b)

Fig. 7. Comparison of (a) solid fraction and (b) PCM mean temperature over time for the straight fins and longitudinal-parabolic fins.

Fig. 8 shows the temperature contours of two cases at different time intervals. The temperature distribution indicates that the solidification process begins nearby the cooling walls and penetrates in the PCM. At initial stages, the temperature of the PCM adjacent to the cooling walls and fins starts to decline till it reaches the PCM liquidus temperature, at which it starts to phase change from liquid to solid state by discharging of thermal energy. As the solidification proceeds and most of the PCM get solidified, more heat transmission results in the decrease of PCM mean temperature until it reaches the temperature of the HTF tube's surface. Temperature contours show that the high temperature regions for the case of straight fins (base case) are more than Case 1 with longitudinal-parabolic fins throughout the discharging process. The temperature reduction in Case 1 is faster than the base case owing to higher thermal penetration depth.

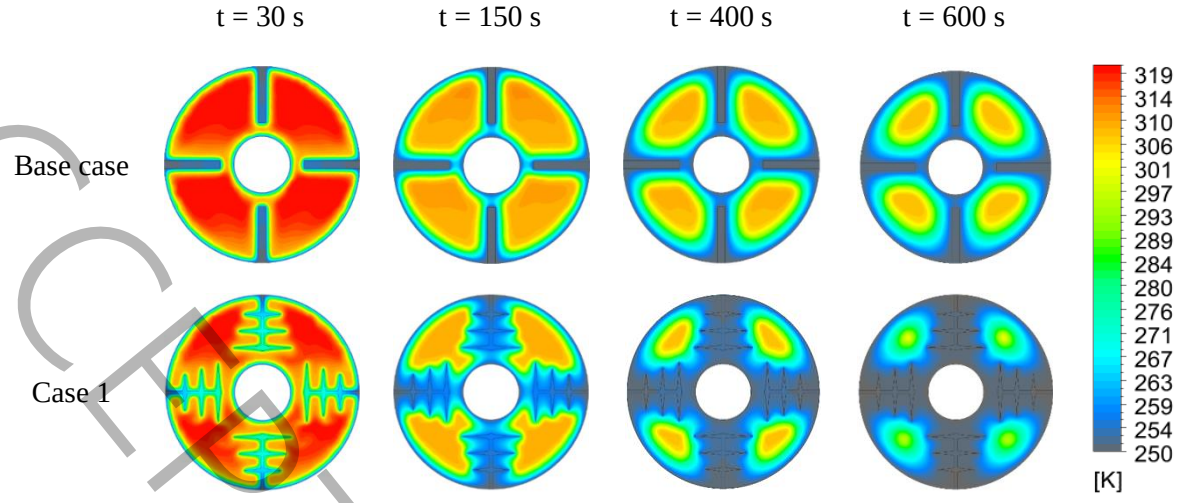

Fig. 8. Temperature contours for two different fin shapes.

4.2. Effect of fin radial pitch on discharging process

Five other longitudinal-parabolic fins with different radial pitches are designed to explore the most effective fin configuration. The fin radial pitches for each case are outlined in Table 2. Fig. 9 illustrates the liquid fraction contours for various cases. Initially, all Cases have similar solidification patterns with solidified PCM concentrated around the shell walls and fins. As time passes, the solidified zone has expanded to the surrounding of the fins. The main difference is observed at the last stage of the discharging process. Cases 1 and 3 could solidify the PCM faster than other cases and Case 4 is the last to complete the solidification. Time changes of the PCM solid fraction correspond to different fin radial pitches are displayed in Fig. 10(a). As can be observed, the solidification rates of six cases are almost the same during initial times. As time goes, Cases 1 and 3 perform better and Case 4 lags behind other cases. The full discharging time difference of Case 3 with Case 1 is only 2s. The full discharging time of Case 3 is 608s and that of Case 4 is 634s. The full solidification time of the cases 1-6 is demonstrated in Fig. 11. It is evident that the differences are small.

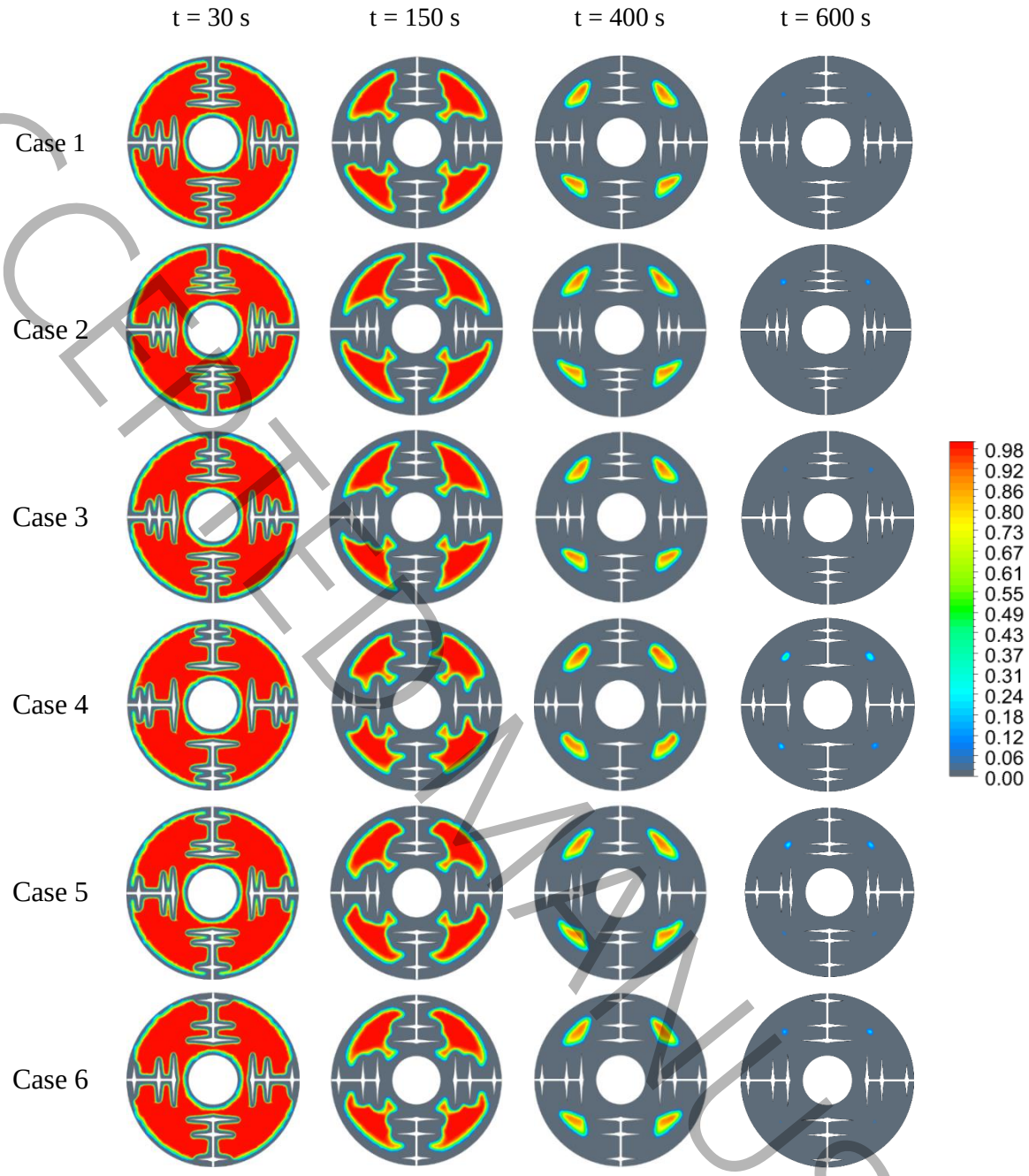

Fig. 9. Liquid fraction contours for different fin radial pitches.

Fig. 10(b) illustrates the PCM mean temperature evolution for various fin radial pitches. It is observed that the slope of the temperature curves is too steep in the early stages of solidification because of the sensible heat removal from the PCM. Over time, once the PCM temperature approaches the liquidus temperature, that signifies the point where it starts transforming from liquid to solid state, the slope of the temperature curves reduces for all

cases. Once the liquidus temperature is reached, a notable phase change occurs within the PCM by absorbing latent heat. The latent heat absorption moderates the rate of temperature decrease. Accordingly, the temperature decline rate through this stage is slower than the initial phase of discharging process. As observed in Fig. 10(b), the reduction of temperature in all cases is close to each other. However, Case 1 and Case 3 show a swifter temperature decline during the heat discharging mode.

Since Case 1 could better enhance the discharging efficiency of the LHTES unit among the examined cases with angular pitch of 90°, this case is considered in the following section to explore the impact of fin angular pitch.

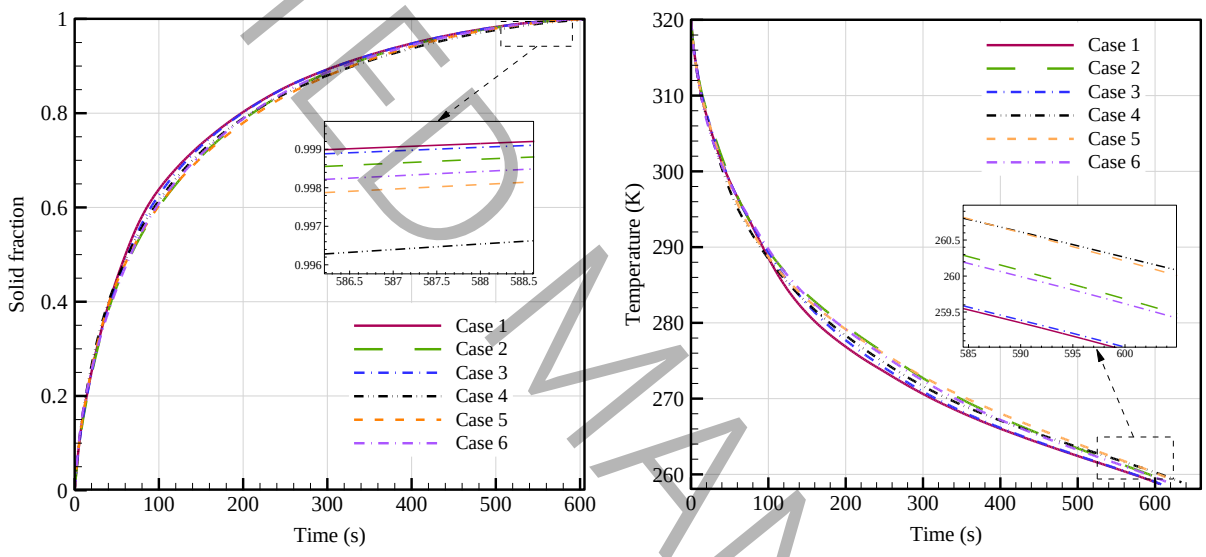

(a) (b)

Fig. 10. Comparison of solid fraction (a) and PCM mean temperature (b) over time for different fin radial pitches.

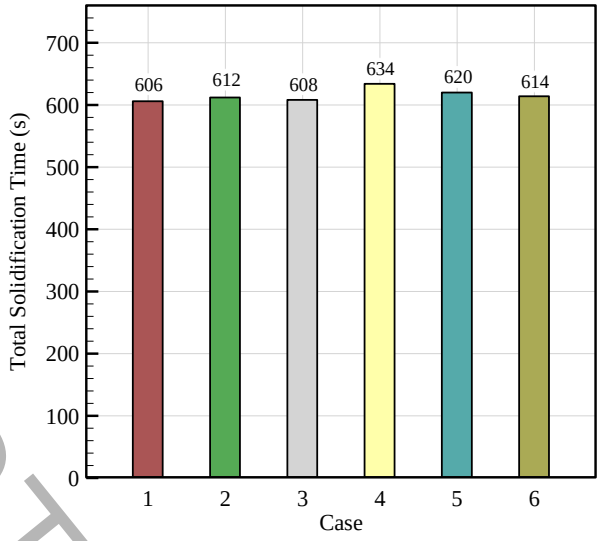

Fig. 11. Solidification times of the cases with various radial pitches.

4.3. Effect of fin angular pitch on discharging process

The influence of angular pitch is also examined to determine the best distribution of the longitudinal-parabolic fins for reducing discharge time. Three different angular pitches are compared while the total cross-sectional area of the fins remains fixed: 120°, 90° and 60°. Fig. 12 displays the liquid fraction contours for different angular pitches at different times. As can be observed, Case 7 with angular pitch of 120° has a slower solidification rate than other cases because the fins are spaced further apart. The solidification speed enhanced by decreasing the angular pitch in Case 1 and Case 8. As the angular pitch decreased from 120° to 60°, contact heat transfer surface with the PCM increased. At t=400s, Case 8 has completed solidification in the entire annulus, while Cases 1 and 7 still contain some liquid PCM. Fig. 13(a) indicates transient evolution of solid fraction for the three angular pitches. It is evident that the solid fraction of Case 8 is higher than those of Cases 1 and 7 because of improving thermal energy transport through the PCM. Using fin configuration with lower angular pitch provides better thermal diffusion and notable reduction in the PCM discharging time throughout the solidification process.

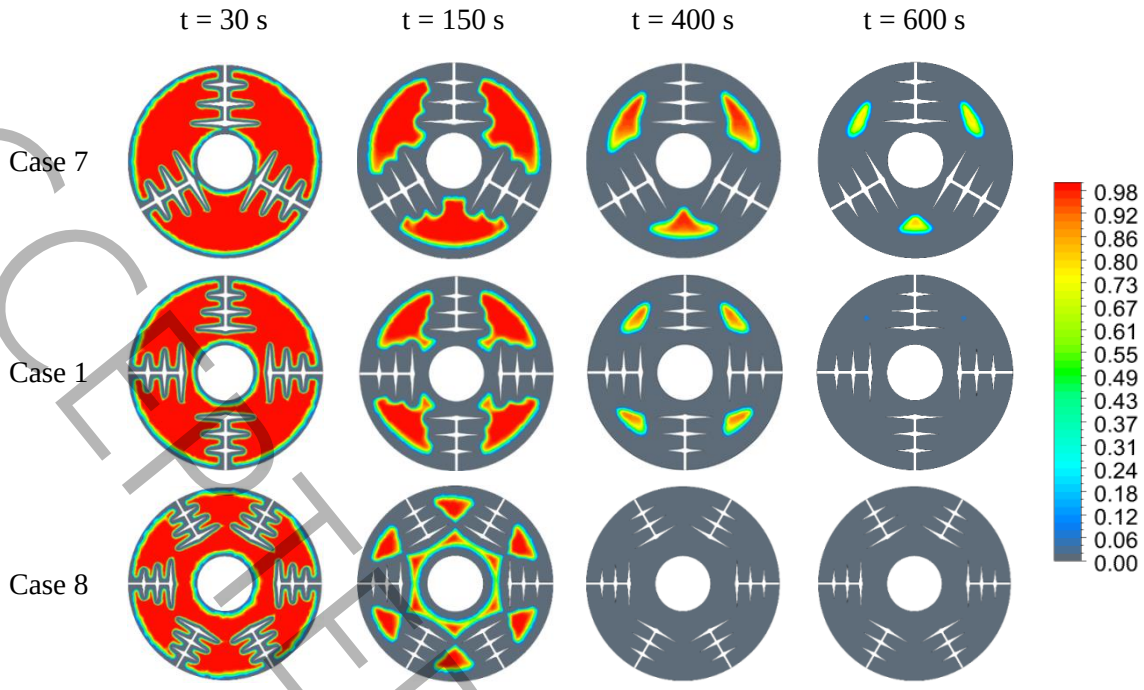

Fig. 12. Liquid fraction contours for different fin angular pitches.

Fig. 13(b) depicts the change of the PCM mean temperate versus time under various fin angular pitches. It reveals that angular pitch of fins has a remarkable influence on the temperature distribution and heat transfer characteristics of the PCM. Reducing the angular pitch causes a faster rate of temperature decrease within the PCM. Case 8 (angular pitch of 60°) completely solidifies after 376s, which is 52.3% less that the time required for Case 7 (angular pitch of 120°). Fig. 14 displays the temperature contour plots of various angular pitches at different time intervals through discharging of PCM. The temperature distribution indicates that decreasing the angular pitch, accelerates the heat transfer rate owing to larger contact surface and facilitates heat dissipation from the PCM over time. Case 8 shows the highest temperature drop rate in the whole process, while Case 7 has the lowest one.

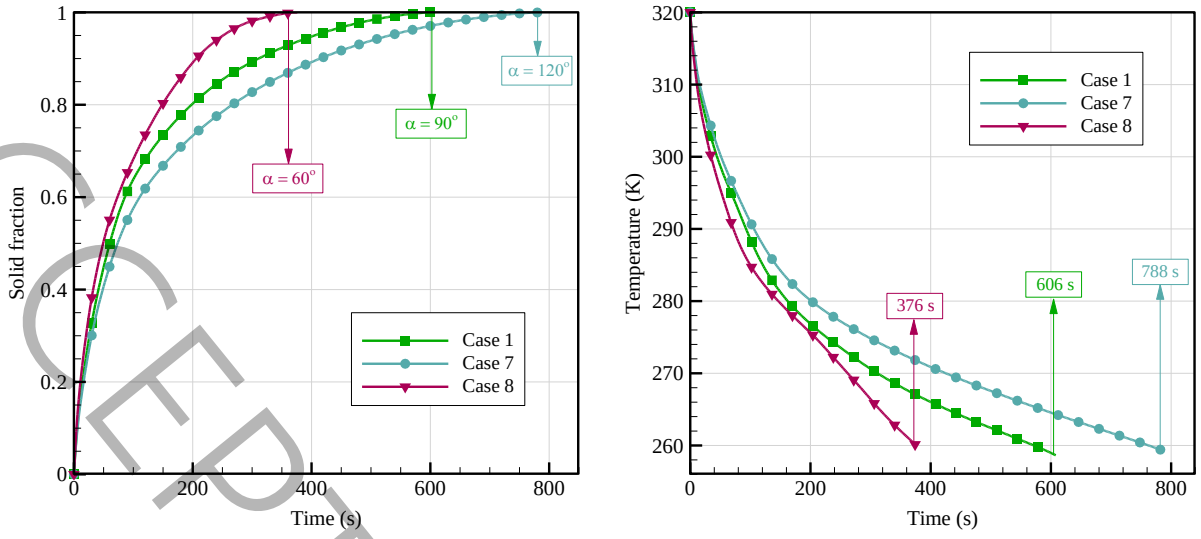

(a) (b)

Fig. 13. Comparing the solid fraction (a) and PCM mean temperature (b) over time for different fin angular pitches.

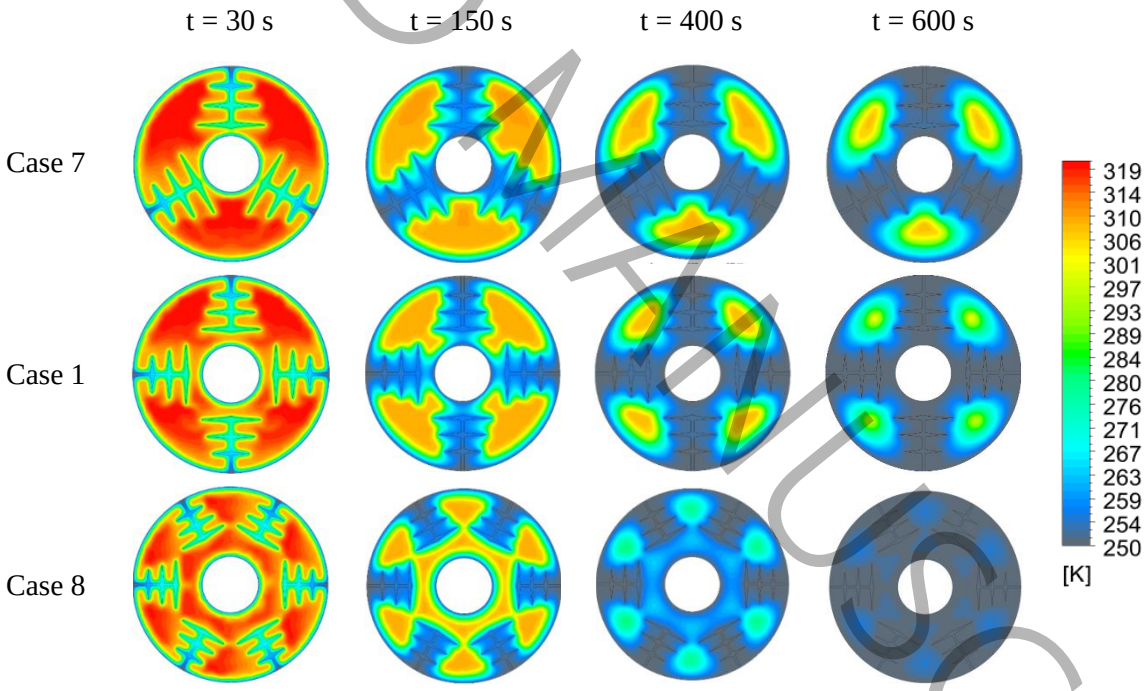

Fig. 14. Temperature contours for different fin angular pitches.

4.4. Comparison of solidification time

The full solidification time for the nine cases is indicated in Fig. 15. The percent reduction in discharging time is represented for the various longitudinal-parabolic fin configurations

relative to the straight fin (the base case). It is obvious that the solidification time is decreased for all the longitudinal-parabolic fin cases in comparison to the straight fin case. For the six different fin radial pitches (Cases 1-6), no significant change in solidification time is observed. However, Case 1 has the minimum discharging time which is 38.54% less than the straight fins case. For the three different fin angular pitches (Case 1-7-8), the full solidification time for Case 8 is minimum which is 37.95% and 52.28% less than Case 1 and Case 7, in respective. Case 8 has the shortest discharging time among the nine cases which is 61.86% less than the base case.

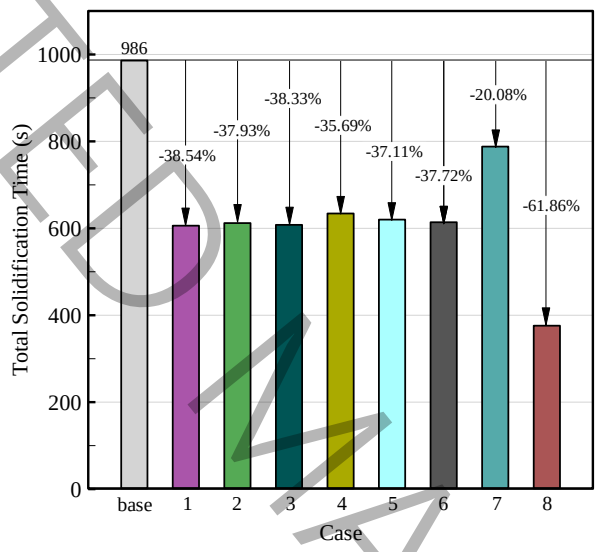

Fig. 15. Complete solidification time for the nine cases.

Conclusion

In the present study, an innovative longitudinal-parabolic fin is embedded into a triplex tube LHTES unit to numerically examine the discharging performance enhancement of PCM. The impacts of geometrical parameters of the designed fin are also investigated to get higher PCM discharging efficiency. The proposed fin is evaluated against the traditional straight fin to reveal its superior thermal performance. Provided that the total surface area of fins holds fixed, several cases with various fin's geometric parameters including radial pitch and angular pitch are examined to find the most efficient fin design for achieving the highest energy discharge efficiency. The conclusions of study are summarized as follows:

- Compared to the traditional straight fins, the complete solidification time of triplex tube LHTES system with the longitudinal-parabolic fins declined up to 38.5% which implies that the new designed fin significantly enhance the PCM discharging rate.
- All of the longitudinal-parabolic fin cases with different radial pitches achieve a reduction in energy discharge time. However, the radial pitches of parabolic fins have little impact on solidification process.
- The angular pitch of longitudinal-parabolic fin has a significant impact on solidification performance, as smaller angular pitches lead to faster discharging rate. By decreasing the angular pitch from 120° to 60°, the solidification time reduces up to 52.3%.
- The maximum of saving discharge time for the most efficient longitudinal-parabolic fin design is 61.8% in comparison with straight fins.

Nomenclature

A_m	mushy constant ($kg.m^{-3}.s^{-1}$)
C_p	specific heat at constant pressure ($J.kg^{-1}.K^{-1}$)
g	gravity acceleration ($m.s^{-2}$)
h	sensible enthalpy ($kJ.kg^{-1}$)
H	total enthalpy ($kJ.kg^{-1}$)
k	thermal conductivity ($W.m^{-1}.K^{-1}$)
L_f	latent heat (MJ)
p	pressure (Pa)
S	momentum source term ($Pa.m^{-1}$)
t	time (s)
T	temperature (K)
u	velocity ($m.s^{-1}$)
Greek symbols	
β	thermal expansion coefficient (K^{-1})
ε	a small number assigned to prevent division by zero
λ	melting fraction
μ	viscosity (Pa.s)
ρ	density ($kg.m^{-3}$)
Subscripts	
l	liquidus of the PCM

ref	reference state
s	solidus of the PCM

Abbreviations

HTF	heat transfer fluid
LHTES	latent heat thermal energy storage
PCM	phase change material
QUICK	quadratic upstream interpolation for convective kinematics
SIMPLE	semi-implicit pressure-linked equations

References

[1] G. Murali, P. Vali, J. Jaya, A.K. Bewoor, R. Kumra, Experimental studies on solar reusable can air heating system integrated with latent heat storage, Journal of Thermal Analysis and Calorimetry, 149 (2024) 8865-8872.

[2] Y. Huo, X. Pang, Z. Rao, Heat transfer enhancement in thermal energy storage using phase change material by optimal arrangement, International Journal of Thermal Science, 161 (2021) 106736.

[3] P. Shahamat, Z. Mehrdoost, Numerical investigation of performance enhancement in a PCM-based thermal energy storage system using stair-shaped fins and nanoparticles, Applied Thermal Engineering, 257 (2024) 124433.

[4] F.L. Rashid, A.K. Hussein, M.A. Al-Obaidi, B.M. Alshammari, B. Ali, R. Hajlaoui, M.M. Boudabous, L. Kolsi, A review of radient heating and cooling systems incorporating phase change materials, Journal of Thermal Analysis and Calorimetry, 149 (2024) 7891-7917.

[5] G. Tang, Y. Lu, S. Shi, F. Wu, L. Tong, S. Zhu, S. Zhang, Z. Wang, X. Guo, Research on the effect and mechanism of composite phase change materials inhibiting low-temperature oxidation of coal, Journal of Thermal Analysis and Calorimetry, 149 (2024) 7635-7649.

[6] Z.A. Qureshi, H.M. Ali, S. Khushnood, Recent advances on thermal conductivity enhancement of phase change materials for energy storage system: A review, International Journal of Heat and Mass Transfer, 127 (2018) 838-56.

[7] K.A.R. Ismail, C.L.F. Alves, M.S. Modesto, Numerical and experimental study on the solidification of PCM around a vertical axially finned isothermal cylinder, Applied Thermal Engineering, 21 (2001) 53-77.

[8] Y. Pahamli, M.J. Hosseini, A.A. Ranjbar, R. Bahrampoury, Effect of nanoparticle dispersion and inclination angle on melting of PCM in a shell and tube heat exchanger, Journal of the Taiwan Institute of Chemical Engineers, 81 (2017) 316-334.
[9] M. Sheikholeslami, Numerical simulation for solidification in a LHTESS by means of nano-enhanced PCM, Journal of the Taiwan Institute of Chemical Engineers, 86 (2018) 25-41.
[10] M. Abdolahimoghadam, M. Rahimi, A numerical evaluation of a latent heat thermal energy storage system in the presence of various types of nanoparticles, Applied Thermal Engineering, 230 (2023) 20854.
[11] Y. Hu, D. Jasim, A. Alizadeh, A. Rahmani, A.S. Al-Shati, M. Zarringhalam, M. Shamsborhan, N. Nasajpour-Esfahani, Simulation of heat transfer in a nanoparticle enhanced phase change material to design battery thermal management systems: A lattice Boltzmann method study, Journal of the Taiwan Institute of Chemical Engineers, 152 (2023) 105137.
[12] Z. Wang, H. Zhang, B. Dou, G. Zhang, W. Wu, X. Zhou, Effect of copper metal foam proportion on heat transfer enhancement in the melting process of phase change materials, Applied Thermal Engineering, 201 (2022) 117778.
[13] B. Wang, J. Xue, Z. Du, J. Yu, L. Lu, T. Xiao, X. Yang, Numerical optimization design of heat storage tank with metal foam for enhancing phase transition, Journal of the Taiwan Institute of Chemical Engineers, 148 (2023) 104466.
[14] R. Hu, X. Huang, X. Gao, L. Lu, X. Yang, B. Sunden, Design and assessment on a bottom-cut shape for latent heat storage tank filled with metal foam, International Journal of Thermal Sciences, 197 (2024) 108575.
[15] M. Sheikholeslami, S. Lohrasbi, D. Domairry Ganji, Response surface method optimization of innovative fin structure for expediting discharge process in latent heat thermal energy storage system containing nano-enhanced phase change material, Journal of the Taiwan Institute of Chemical Engineers, 67 (2016) 115-125.
[16] R. Hamid, Z. Mehrdoost, Thermal performance enhancement of multiple tubes latent heat thermal energy storage system using sinusoidal wavy fins and tubes geometry modification, Applied Thermal Engineering, 245 (2024) 122750.
[17] Y. Shen, A.R. Mazhar, P. Zhang, S. Liu, Structure optimization of tree-shaped fins for improving the thermodynamic performance in latent heat storage, International Journal of Thermal Sciences, 184 (2023) 108003.

[18] Z. Zhang, Z. Zhu, Thermodynamic performance improvement of the horizontal shell-and-tube latent heat thermal storage unit by splitter plates and upper-and-lower cascade PCM, Journal of Energy Storage, 83 (2024) 110802.
[19] S. Nekoonam, R. Roshandel, Modeling and optimization of a multiple (cascading) phase change material solar storage system, Thermal Science and Engineering Progress, 23 (2021) 100873.
[20] Z. Liu, Z. Liu, J. Guo, F. Wang, X. Yang, J. Yan, Innovative ladder-shaped fin design on a latent heat storage device for waste heat recovery, Applied Energy, 321 (2022) 119300.
[21] A. Sciacovelli, F. Gagliardi, V. Verda, Maximization of performance of a PCM latent heat storage system with innovative fins, Applied Energy, 137 (2015) 707-715.
[22] M. Sheikholeslami, S. Lohrasebi, D.D. Ganji, Numerical analysis of discharging process acceleration in LHTESS by immersing innovative fin configuration using finite element method, Applied Thermal Engineering, 107 (2016) 154-166.
[23] K.A. Aly, A.R. El-Lathy, M.A. Fouad, Enhancement of solidification rate of latent heat thermal energy storage using corrugated fins, Journal of Energy Storage, 24 (2019) 100785.
[24] S. Zhang, L. Pu, L. Xu, R. Liu, Y. Li, Melting performance analysis of phase change materials in different finned thermal energy storage, Applied Thermal Engineering, 176 (2020) 115425.
[25] Y. Huang, X. Liu, Charging and discharging enhancement of a vertical latent heat storage unit by fractal tree-shaped fins, Renewable Energy, 2174 (2021) 199-217.
[26] S. Yao, X. Huang, Study on solidification performance of PCM by longitudinal triangular fins in a triplex-tube thermal energy storage system, Energy, 227 (2021) 120527.
[27] X. Huang, S. Yao, Solidification performance of new trapezoidal longitudinal fins in latent heat thermal energy storage, Case Studies in Thermal Engineering, 26 (2021) 101110.
[28] J.R. Patel, M.K. Rathod, M. Sherement, Heat transfer augmentation of triplex type latent heat thermal energy storage using combined eccentricity and longitudinal fin, Journal of Energy Storage, 50 (2022) 104167.
[29] Z. Zheng, X. Cai, C. Yang, Y. Xu, Improving the solidification performance of a latent heat thermal energy storage unit using arrow-shaped fins obtained by an innovative fast optimization algorithm, Renewable Energy, 195 (2022) 566-577.
[30] L. Lijun, N. Yaqian, L. Xiaoqing, L. Xiaoyan, Numerical simulation of the improvement of latent heat storage unit performance in solidification process by eccentric fractal finned tube, Journal of Energy Storage, 57 (2023) 106044.

[31] J. Zhang, Z. Cao, S. Huang, X. Huang, Y. Han, C. Wen, J. Honoré Walther, Y. Yang, Solidification performance improvement of phase change materials for latent heat thermal energy storage using novel branch-structured fins and nanoparticles, Applied Energy, 342 (2023) 121158.
[32] F. Ma, T. Zhu, Y. Zhang, X. Lu, W. Zhang, F. Ma, A Review on Heat Transfer Enhancement of Phase Change Materials Using Fin Tubes, Energies, 16 (2023) 545.
[33] Y. Amini, M.H. Abbasirad, Melting performance enhancement of a latent thermal energy storage device using innovative arc fins and nanoparticles, Journal of Brazilian Society of Mechanical Sciences and Engineering, 45 (2023) 298.
[34] C. Li, Q. Li, R. Ge, Assessment on the melting performance of a phase change material based shell and tube thermal energy storage device containing leaf-shaped longitudinal fins, Journal of Energy Storage, 60 (2023) 106574.
[35] A. Tavakoli, M. Farzaneh-Gord, A. Ebrahimi-Moghadam, Using internal sinusoidal fins and phase change material for performance enhancement of thermal energy storage systems: Heat transfer and entropy generation analysis, Renewable Energy, 205 (2023) 222-237.
[36] S. Baghaei Oskouei, O. Bayer, Experimental and numerical investigation of melting and solidification enhancement using Fibonacci-inspired fins in a latent thermal energy storage unit, International Journal of Heat and Mass Transfer, 210 (2023) 124180.
[37] Z.J. Zheng, H. Yin, C. He, Y. Wei, M. Cui, Y. Xu, Parameter optimization of unevenly spiderweb-shaped fin for enhanced solidification performance of shell and tube latent-heat thermal energy storage units, Journal of Energy Storage, 30 (2023) 108495.
[38] M. Boujelbene, H.I. Mohammed, H.S. Sultan, M. Eisapour, Z. Chen, J.M. Mahdi, A. Cairns, P. Talebizadehsardari, A comparative study of twisted and straight fins in enhancing the melting and solidifying rates of PCM in horizontal double-tube heat exchangers, International Communications in Heat and Mass Transfer, 151 (2024) 107224.
[39] H. Li, C. Hu, D. Tang, Z. Rao, Improving heat storage performance of shell-and-tube unit by using structural-optimized spiral fins, Journal of Energy Storage, 79 (2024) 110212.
[40] M. Sheikholeslami, A. Nematpour Keshteli, A. Shafee, Melting and solidification within an energy storage unit with triangular fin and CuO nanoparticles, Journal of Energy Storage, 32 (2020) 101716.
[41] V.R. Voller, C. Prakash, A fixed grid numerical modeling methodology for convection diffusion mushy region phase change problems, International Journal of Heat and Mass Transfer, 30 (1978) 1709-1719.
[42] ANSYS Academic Research, "ANSYS fluent theory guide," 2019.

[43] A.D. Brent, V.R. Voller, K.J. Reid Enthalpy-porosity technique for modeling convection-diffusion phase change: application to the melting of a pure metal, Numerical Heat Transfer, 13 (1988) 297-318.

[44] F.L. Tan, S.F. Hosseinzadeh, J.M. Khodadadi, L. Fan, Experimental and computational study of constrained melting of phase change materials (PCM) inside a spherical capsule, International Journal of Heat and Mass Transfer, 52 (2009) 3464-3472.

[45] A.A. Al-Abidi, S. Mat, K. Sopian, M.Y. Sulaiman, A.T. Mohammad, Experimental study of melting and solidification of PCM in a triplex tube heat exchanger with fins, Energy and Buildings, 68 (2014) 33-41.